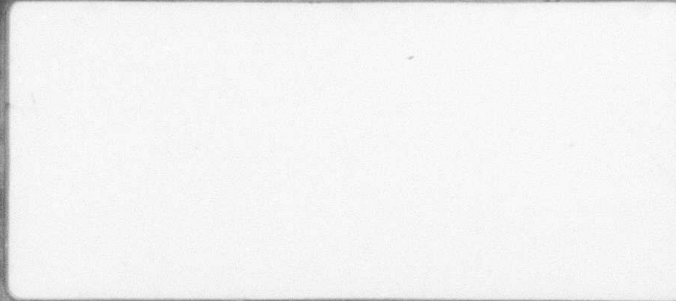


#3/1/14

90 2267

ADA112754

①



Abex
CORPORATION

RESEARCH CENTER
MAHWAH, NEW JERSEY

DTIC FILE COPY

DTIC
SELECTE
S APR 1 1982
A

This document has been approved
for public release and sale; its
distribution is unlimited.

82 03 30 076

Abex

Abex Corporation
An IC Industries Company

Research Center

MANWAN, NEW JERSEY 07430

TEL: 201-529-3450

APPROVED FOR PUBLIC RELEASE
DISTRIBUTION UNLIMITED
ANNUAL TECHNICAL REPORT

ARPA CONTRACT NO. DAAG46-73-C-0113

MACHINE CASTING OF FERROUS ALLOYS

FR-AD-A034198

DTIC
S ELECTE D
APR 1 1982
A

82 03 30 076



Abex Corporation
An IC Industries Company

Research Center

MAHWAH, NEW JERSEY 07430

TEL: 201-529-3450

ANNUAL TECHNICAL REPORT
ARPA CONTRACT NO. DAAG46-73-C-0113
MACHINE CASTING OF FERROUS ALLOYS

FEBRUARY 1974

Project Scientist: Dr. H.R. Larson (Tel:201-529-3450)

Principal Investigator: Dr. C.P. Biswas (Tel:201-529-3450)

Abex Corporation
Research Center
Mahwah, N.J. 07430

Sponsored by: Advanced Research Projects Agency
ARPA Order No. 2267

Program Code No.: 61101E

Effective Date of Contract: February 1, 1973

Contract Expiration Date: December 31, 1973

Amount of Contract: \$139,075.00

DTIC
ELECTE
S APR 1 1982 D
A

The views and conclusions contained in this document are those of the authors and should not be interpreted as necessarily representing the official policies, either expressed or implied, of the Advanced Research Project, Agency of the U.S. Government.



SUMMARY

Accession For	DTIC GRA&I	<input checked="" type="checkbox"/>	<input type="checkbox"/>	<input type="checkbox"/>
	DTIC TAB			
	Unannounced			
	Justification			
By	Distribution/			
	Availability Codes			
	Avail and/or			
	Dist Special			
				A

The work at Abex Corporation during the first year of the contract has been directed toward three primary objectives: (1) design and construction of a pilot casting machine capable of evaluating rheocasting as well as more conventional casting techniques, (2) development of a magnetohydrodynamic valve for controlling metal flow, and (3) development of a mold material capable of withstanding the rigors of the machine casting of ferrous metals.

A pilot casting machine has been designed and is under construction. In some ways, this machine is intended to be the forerunner of a full scale production apparatus. However, its immediate objective will be to evaluate the Rheocasting process with respect to processing and properties. The melting and casting operation will take place entirely under an inert atmosphere at low positive pressure to minimize slag formation. The transfer of the metal "slurry" to the mold is accomplished by pressurizing the chamber to 100 psi and retracting a bottom pouring plug while the stirring paddles are still on. The design of the casting unit will permit the subsequent inclusion of an MHD valve if desireable and, in addition, can be operated with conventional superheated liquid metal as well as semi-solid Rheocast metal.

Abex's work on MHD valving has demonstrated that some lift can be obtained from an MHD conduction device to hold the bulk metal, and to control its flow. However, much stronger lift force is required for any practical casting machine. Also, the basic problem that remains is stabilization of the lower metal-air interface that causes the value to leak. Work is being done to produce a stronger levitation force and stabilize the interface by using various coil designs and power supply of various powers, frequencies and phases.

With the outstanding exception of its poor resistance to oxidation and erosion by ferrous alloys, graphite has most of the attributes of an ideal mold material. Abex's effort, therefore, has been concentrated on producing a coating that will protect the graphite surface. For the formation of protective coating different approaches have been taken like, plasma spraying, metallizing with subsequent diffusion annealing and hot pressing. Although the experiments are still in progress, the most promising approach thus far involves the formation of metallic carbide on the graphite surface and subsequently plasma spraying with zirconia to provide the final mold surface. Among all the ceramic materials we have examined so far, hot pressed silicon nitride has shown considerable promise.

REPORT

This report presents the work done at Abex Corporation during the first year of a program designed to develop a ferrous casting system that will produce quality castings at a higher speed and lower cost than is possible by present casting methods. The work has been done primarily on the following topics:

- (1) Design and Fabrication of a Pilot Melting and Casting Unit;
- (2) Development of a Magnetohydrodynamic (MHD) Valve to Control and Stop Metal Flow;
- (3) Development of a Permanent Mold.

(1) Design and Fabrication of a Pilot Melting and Casting Unit.

Design and fabrication of a pilot melting and casting unit was undertaken with four specific objectives in mind:

- a. Evaluation of conventional vs. rheocasting processing, and development of systems, parameters for either or both approaches.
- b. Determination of the mechanical properties of rheocast metal: cast iron and, ultimately, steel.
- c. Evaluation of the design and the materials of construction in the casting unit and the mold, particularly those materials in close proximity to or contact with the molten metal.

(1) Contd.

- d. Testing of an MHD valve should it become a feasible device.

The casting unit was designed on the basis of several fundamental requirements of the Rheocasting Process, as well as other features considered to be generally desirable for a conventional casting process. The following is a partial list of these basic requirements.

- a. The melting and casting operation should take place entirely under an inert atmosphere to minimize slag attack and other problems associated with the presence of an air environment.
- b. The melt must be stirred continuously from the point at which the liquidus temperature is achieved to the point at which the casting operation begins.
- c. The metal containing some predetermined fraction of solid must be moved rapidly and forcefully from the melting crucible into the mold, maintaining, as much as possible, the stirring action throughout the casting operation.

Figure (1) shows the details of the Abex casting unit that is designed to meet these requirements. The materials from which the unit is being constructed are as follows:

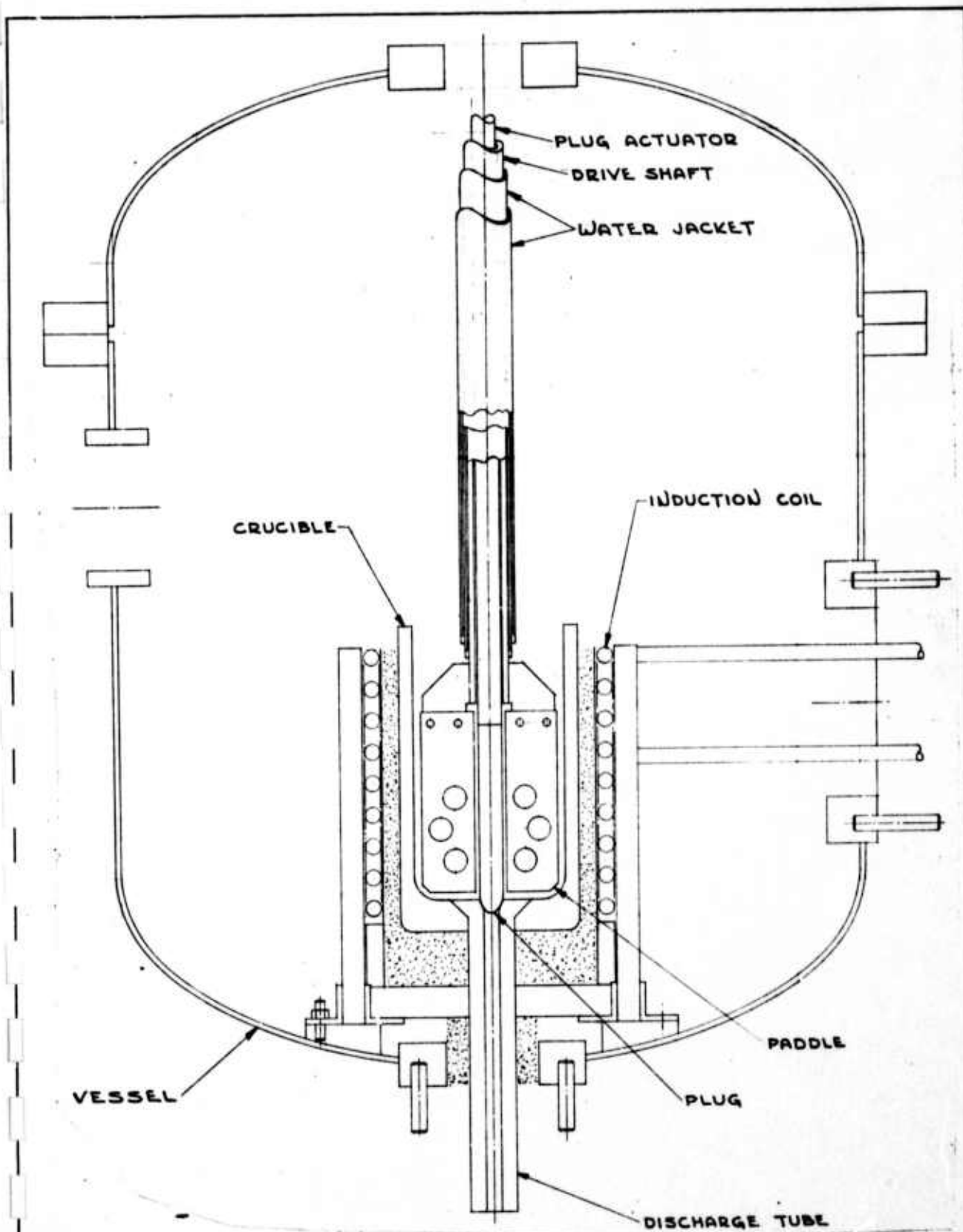


Figure 1

				MANUFACTURING RESEARCH AND DEVELOPMENT	
		MAHWAN N. J. 07430			
FURNACE & VESSEL ARRANGEMENT					
DES.	DR. J. M.	CH.	DATE		
MATERIAL		EST. WEIGHT RAW FIN.	SCALE	1'	SHEET OF
					D

(1) contd.

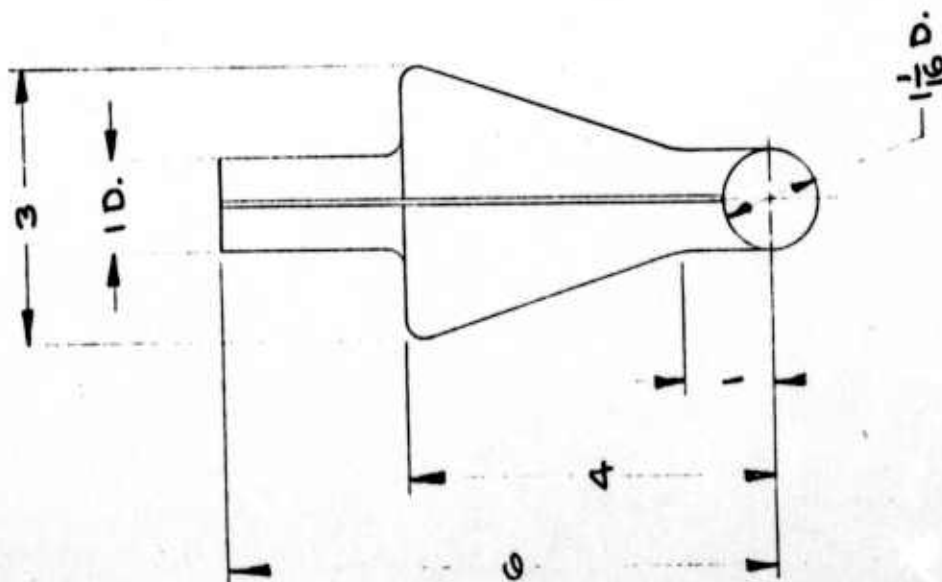
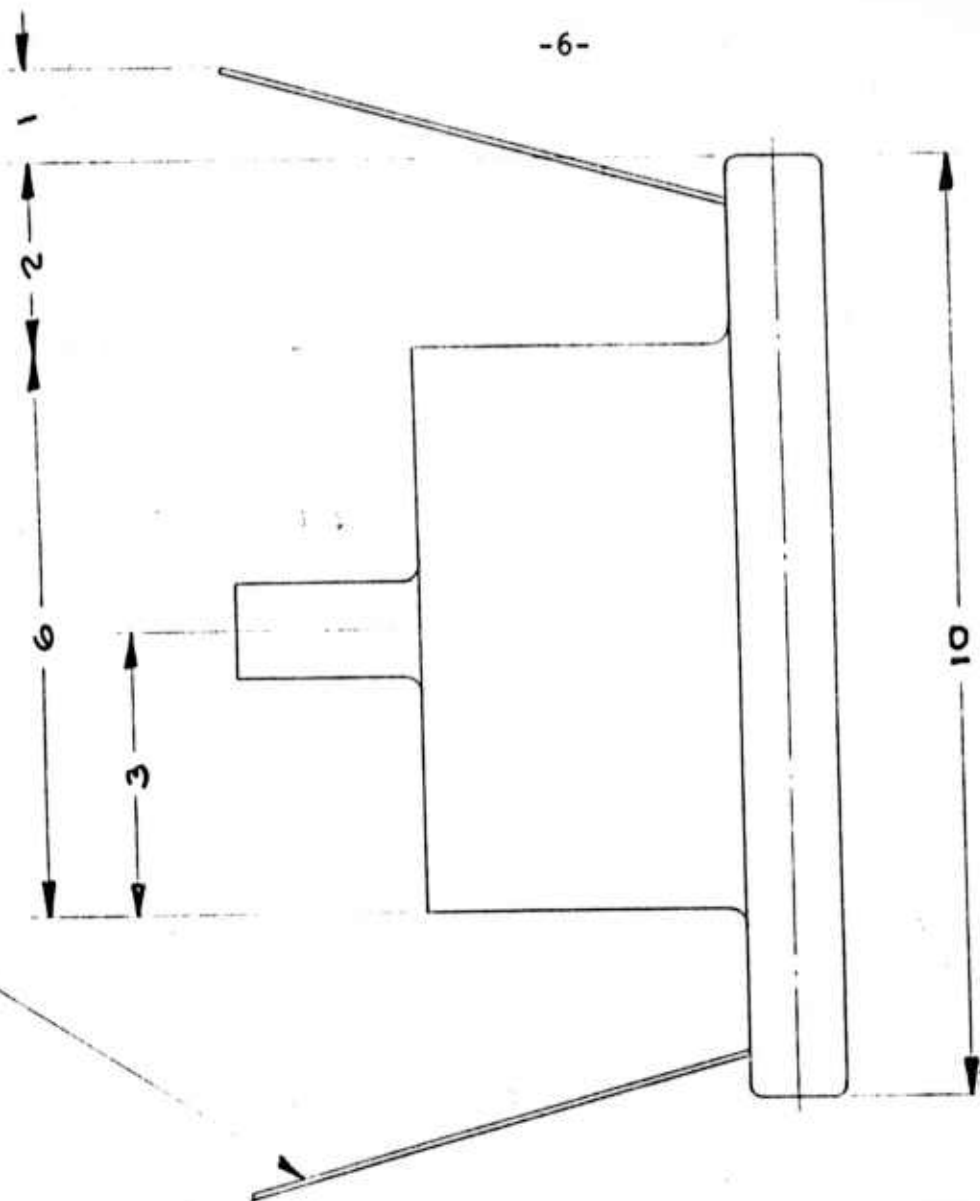
<u>Component</u>	<u>Materials</u>
Pressure Vessel (Fig. 2)	Austenitic stainless steel weld fabrication.
Melting Unit (Fig. 1)	Conventional induction melting coils with special support construction for mounting and bottom pour. Power - 100KW Frequency - 3000 cps Source - M.G. Set
Bottom Plug (Fig. 4)	Alumina
Plug Actuator (Fig. 1)	Austenitic stainless steel.
Drive Shaft (Fig. 1)	Austenitic stainless steel.
Crucible (Fig. 5)	Alumina
Stirring Paddles (Fig. 6)	Alumina and/or silicon oxynitride.
Discharge Tube (Fig. 7)	Alumina
Drive Motor (not shown)	Conventional motor of sufficient power, etc.

Figure (2) shows the pressure vessel in greater detail, including sight ports, access ports, etc.

The molds for the casting unit will be graphite, and will eventually be coated according to the results of the "Mold Materials" program in progress concurrent with the cast-

Figure 2

$\frac{1}{16}$ DIA. VENTS (OPTIONAL)

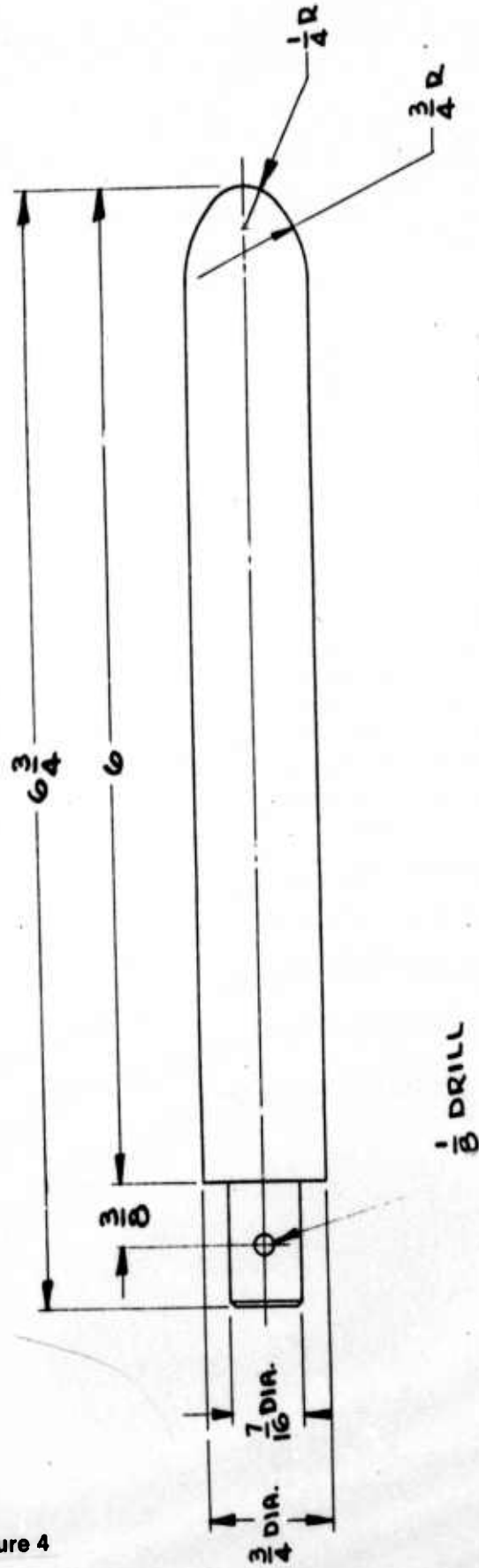


-6-

ABEX TEST BAR DIA 14

Figure 3

Figure 4



Abex		MANUFACTURING RESEARCH AND DEVELOPMENT MAHWAH, N. J. 07430	
PLUG ARPA PROJECT			
DES.	DR. J.M.	CK.	DATE 10-27-73
SHEET OF		1928-04	
SCALE: $\frac{1}{8} = 1'$		EST. WEIGHT RAW FIN.	
MATERIAL		B	

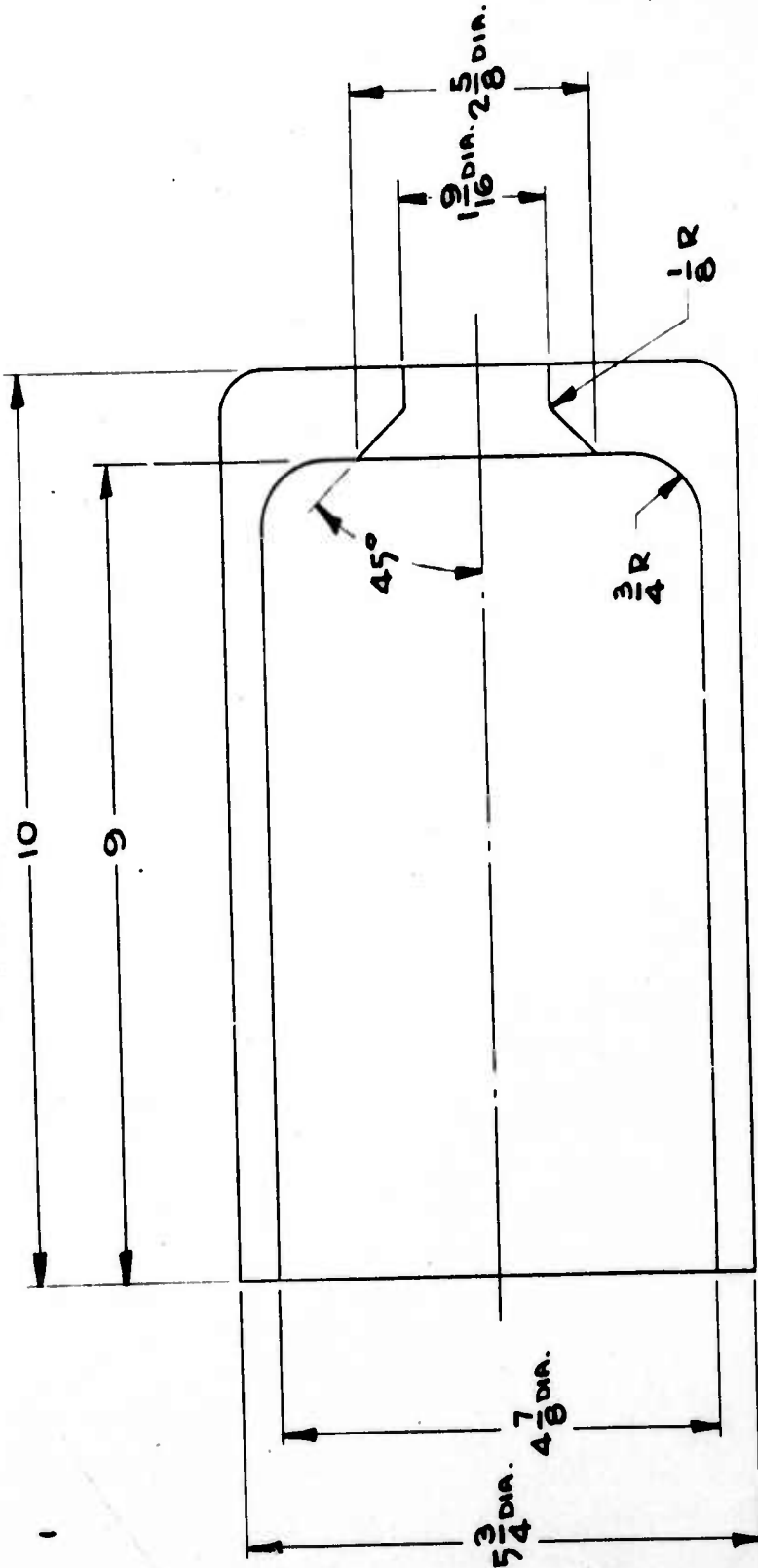
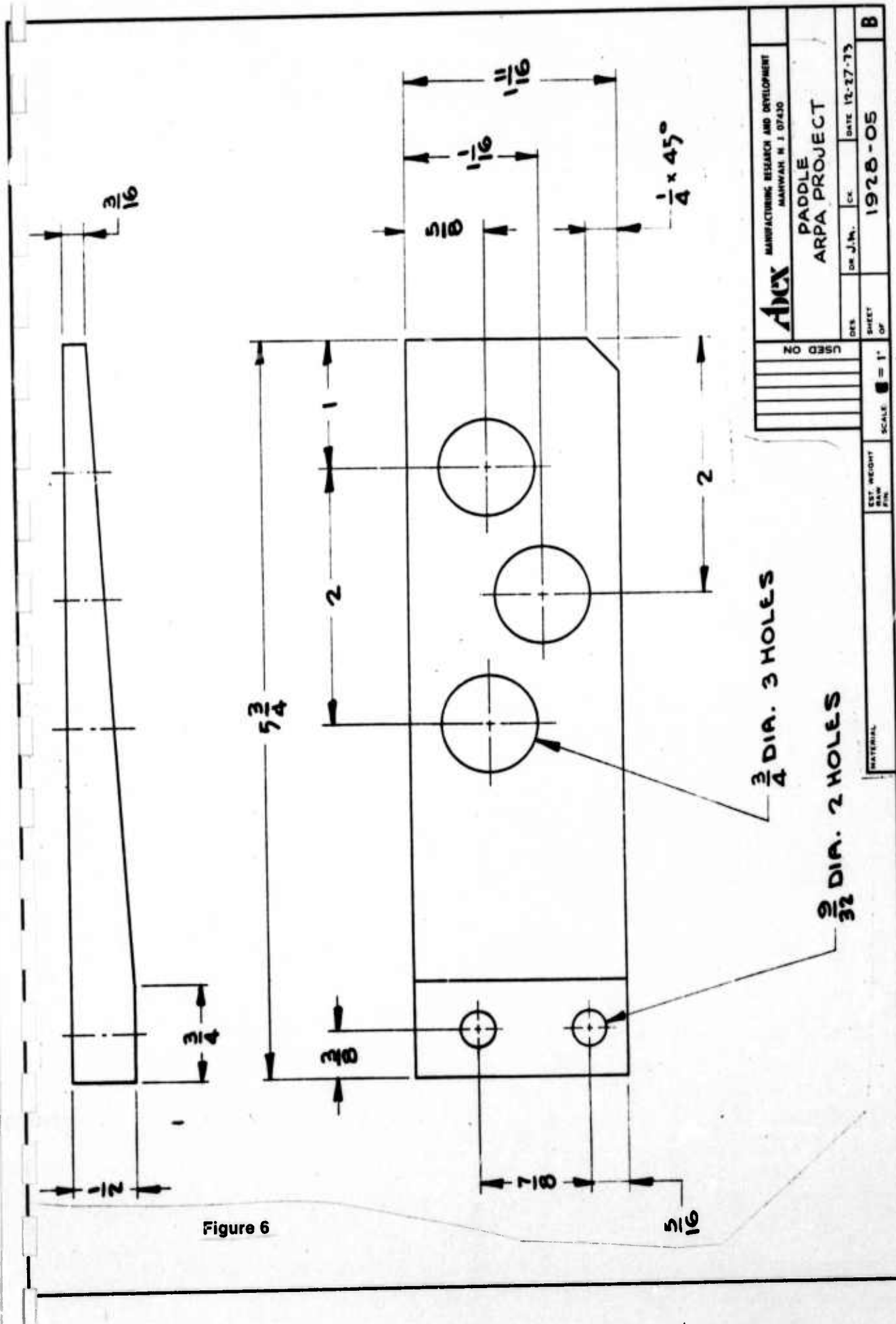


Figure 5

Apex MANUFACTURING RESEARCH AND DEVELOPMENT MANHATTAN N. Y. 10740		DES. <input type="checkbox"/> CK. <input type="checkbox"/> DATE 12-18-73		SHEET OF <input type="checkbox"/>
USED ON <input type="checkbox"/>		OR J.N. <input type="checkbox"/>		
MATERIAL <input type="checkbox"/>		SCALE <input type="checkbox"/> = 1"		1928-02
WEIGHT <input type="checkbox"/>		PIN <input type="checkbox"/>		
B		B		B



(1) contd.

ing unit construction. The first castings to be produced will be a test bar as shown in Figure (3). This bar design has been used for many years by the Abex Experimental Foundry for the evaluation of alloys and processes, and its foundry characteristics are well documented.

The casting process for this pilot casting unit has been outlined as follows:

- (1) With the chamber open, charge the appropriate alloys to the melting unit with the paddle in the raised position and the plug in the sealed position.
- (2) Close chamber and flush with inert gas.
- (3) Melt down under slight positive pressure of inert gas.
- (4) Adjust temperature to just above liquidus, lower paddle into melt, and begin stirring. Paddle-to-crucible clearance of 1/4" per side will provide the shear required for Rheocasting.
- (5) Cool the melt to the appropriate temperature below the liquidus corresponding to the fraction solid desired.

(1) contd.

- (6) Pressurize the chamber to a positive pressure up to 100 psi (as required).
- (7) Pull bottom plug to cast into previously positioned mold. Mold may or may not be evacuated.

This unit will process one 20 lb. casting each melting and casting cycle. The data obtained from operation of this unit should, however, provide much of the input required to design a multi-casting or semi-continuous unit for full scale production.

At this writing, all design work has been completed on the pilot casting unit, and fabrication is progressing as ordered components are received.

(2) Development of a Magnetohydrodynamic (MHD) Valve to Control and Stop Metal Flow.

This phase of the ferrous casting project calls for the investigation to determine the feasibility of using magnetohydrodynamic force as a valve to control and stop metal flow. This electromagnetic valve will circumvent many of the mechanical and materials problems associated with existing pouring methods - stopper rod valve, slide gate valve, etc. The control or complete stoppage of flow can be accomplished by magnetodynamic pinch-off of flow, or, by the magnetohydrodynamic countering of the force of gravity through use of a gravity decelerator.

(2) contd.

The basic force in an MHD device can be expressed by

$$\vec{F} = \vec{J} \times \vec{B} \quad (1)$$

where, F is the force experienced by the liquid

J is the current density

B is the magnetic flux density

There are two kinds of MHD device of interest, conduction and induction types. In the conduction type, a direct current is applied through the liquid, whereas, in the induction type, the current is induced in the liquid by an external induction field.

In a conduction cell, the static support of a vertical column of liquid against the gravity is given by the relation,

$$JB = \rho gh \quad (2)$$

where, ρ is the mass density of the liquid

g is the acceleration due to gravity

h is the height of the liquid column

In an induction cell, on the other hand, the static support of a liquid column is given by,

$$B^2/2\mu_0 = \rho gh \quad (3)$$

where, $\mu_0 = 12.57 \times 10^{-7}$ in MKS units

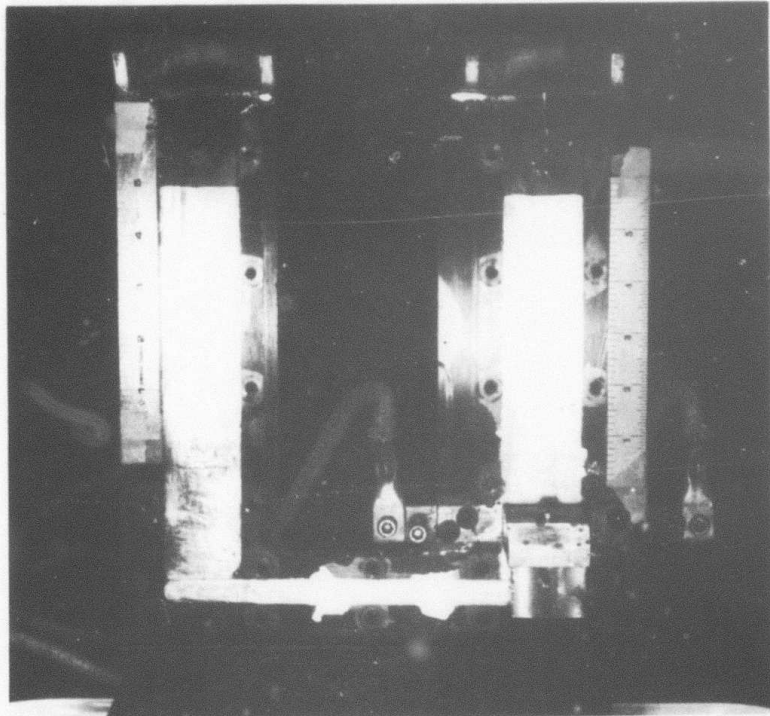
On the basis of equations 2 and 3, calculations have showed that the suspension of a sizeable head of molten iron is feasible by using magnetohydrodynamic forces.

(2) contd.

The preliminary experiments of both conduction and induction type MHD valves have been done, and it was found that a reasonable lifting force can be generated by the MHD device, but the major problem is the instability of the metal-air interface, and therefore, a tendency for the valve to leak.

The set up for the conduction type experiment is shown in Figure 8. It consists of a plexiglass U-tube with a conduction pump installed in one leg. The cross section of the cavity is rectangular with 1.5" x 0.05" sides. Mercury was used as the liquid medium. A current varying from 0 to 150 amps was applied along the long sides of the cavity and a magnetic field of about 2,000 gauss was applied by a permanent magnet along the short sides and the MHD force generated thereby was vertical.

The MHD force generated was found to be proportional to the applied current as shown in Figure 9. The graph also shows the theoretical force that was calculated on the basis of uniform current and flux density. The discrepancy is due to fringing of the electrical and magnetic fields leading to non-uniform field densities, and also energy lost due to heating of mercury. This heating was, fortunately, very minor.



MHD Conduction Pump Experiment

Figure 8

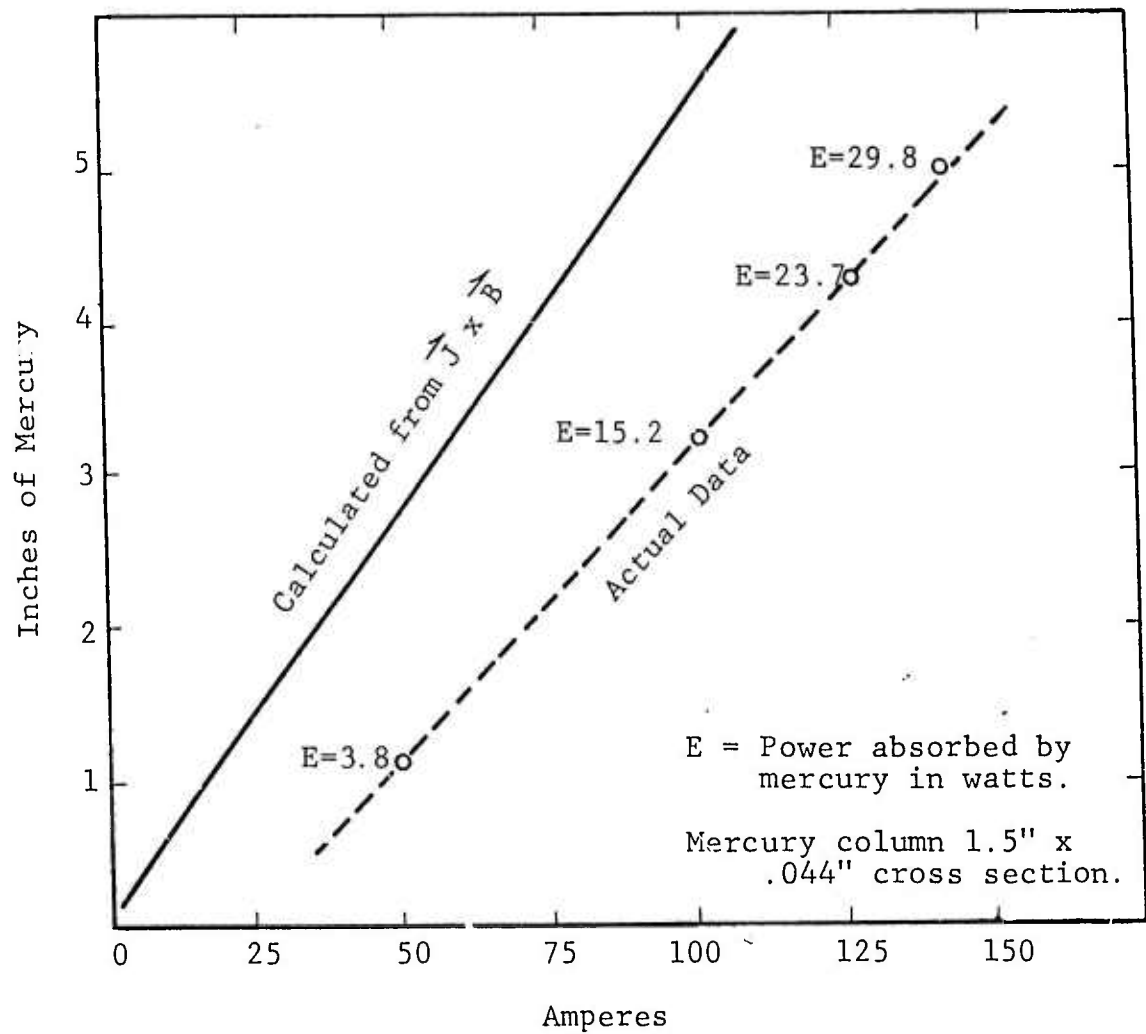


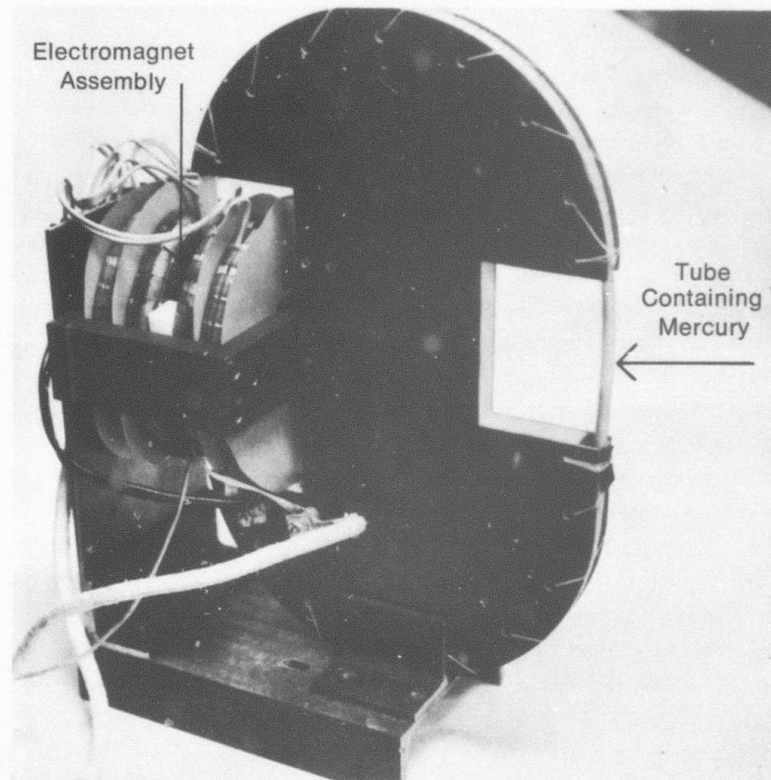
Figure 9. Theoretical and actual performance of conduction pump.

(2) contd.

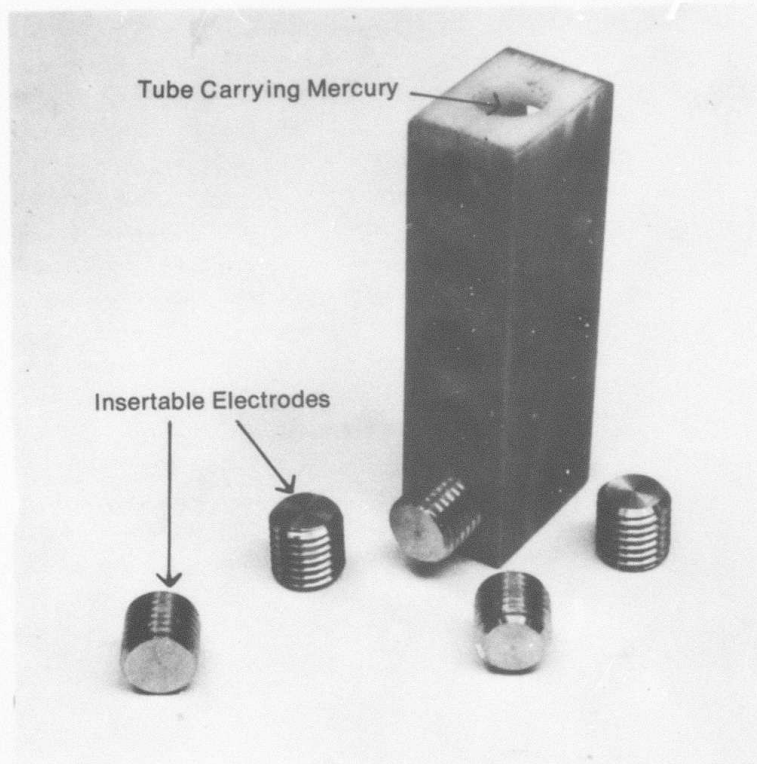
The stability of the mercury-air interface was investigated by attempting to pump the mercury above as well as below the electrode contacts. In both cases the liquid surface was unstable.

It was realized that a stronger magnetic field was necessary for levitation of any practical importance. Therefore, an improved conduction cell was designed and built (Figure (10)) in which an electromagnet capable of producing 4,000 gauss field, and also a circular cross section tube with round insertable multiple electrodes (Figure 11) were used. The circular geometry was selected because of its conformity to a practical refractory nozzle. The test of this apparatus indicated no appreciable difference in the lift obtained from the first experiment. This was due to considerable power loss in the electromagnet structure and, therefore, its inability to attain the design value of magnetic flux. The current required was approximately 40 amps per c.c. of mercury per kilograms at 3.7 watts per c.c. at the electrodes.

In the induction type experiment woods metal was used in a 0.5" diameter pyrex tube. The current was supplied from a 10 KW, 610,000 Hertz power source into a 6 turn induction coil placed around the tube. Although



MHD Conduction Cell Electromagnet
Figure 10



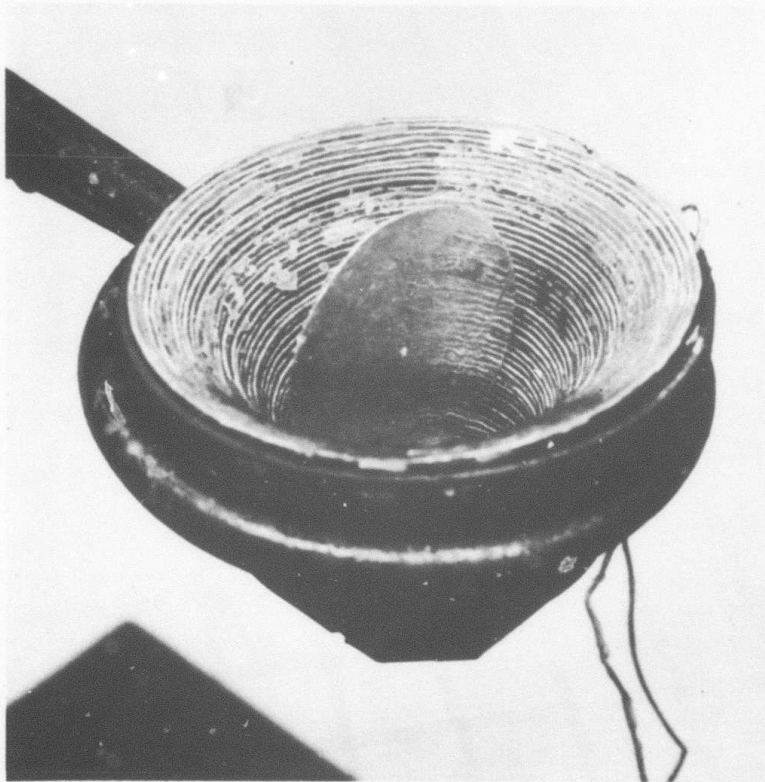
Multiple Electrode Assembly
Figure 11

(2) contd.

the MHD force supported a small column of liquid, the metal trickled through at the center. This leak was due to the absence of any vertical force at the center. Therefore, for an efficient lifting of the liquid throughout the cross section we need an induced magnetic field that will produce stress fields with strong vertical components at all points. This can be achieved by using a conical induction coil that is capable of producing magnetic fields with strong horizontal components at each point in the liquid. The achievement of levitation has been obtained in the past through use of this type of tapered coil configurations.

Accordingly, we built a conical levitation coil assembly that is shown in Fig. 12. A copper plated ping pong ball was used for levitation. When resonated with 0.01 mfd at 17 kHz, the heating of the plating occurred without any levitation. No levitation could be achieved up to a 150 volt-amp power. Aluminum and copper discs and hoops of 1" to 1-1/2" dia. were also tried for levitation, but the coil either propels or turns them on their ends, but does not hold them levitated. Experiments using different power supply with different frequencies are still in progress.

Besides generating a magnetic field with strong horizontal component, the magnitude of induced current and its penetration depth are equally important for successful



Levitation Coil

Figure 12

(2) contd.

levitation. These factors are governed by the frequency of the power supply. A higher frequency field generates a stronger eddy current, shallower skin depth and consequently more heating and less levitation of the melt. Theoretical and experimental investigations are being made of the partitioning characteristics between levitation and heating.

Okress and Wroughton (1) of Westinghouse Electric Co. made a thorough investigation of the levitation phenomena making use of tapered fields having conical and pancake geometry. The force relation derived by Okress et al is:

$$F = KI^2 m/d \cdot G(x) \quad (4)$$

where, K = a geometrical constant

I = coil current

m/d is ratio of charge-mass to density
to the charge

$$G(x) = 1 - \frac{3}{4x} \frac{(\sinh 2x - \sin 2x)}{(\sinh^2 2x + \sin^2 2x)} \quad (5)$$

where, $x = a/\delta$, the ratio of charge radius (a sphere is implied) to skin depth and

$$\delta = \left(\frac{2}{\omega \sigma \mu} \right)^{\frac{1}{2}} = \left(\frac{1}{\pi f \sigma \mu} \right)^{\frac{1}{2}} \quad (6)$$

where, $\omega = 2\pi f$, the angular frequency applied

σ is the conductivity of the charge

μ is the relative permeability of the charge

(2) contd.

Little is known about the function $G(x)$, although it has been plotted as a function of a/δ and frequency as shown in Fig. 13. Fig. 14 shows the relation between the resistance factor of induction heating, K_r and $2a/\delta$.

Fromm and Jehn (2) derived the formula for heating effect attendant to a levitation situation and it is given by

$$N = 3 \pi a H_p^2 F_1(x) \quad (7)$$

In the frequency range where $a/\delta = 10$, this relation becomes

$$N = 3 \pi p a^2 H^2 / \delta = 3 (\pi^3 \mu)^{\frac{1}{2}} (fp)^{\frac{1}{2}} a^2 H^2 \quad (8)$$

A plot of $F_1(x)$ and $G(x)$ is shown in Fig. 15.

Fig. 16 shows that for the same a/δ value, a hollow work piece gives a higher value of $G(x)$ than a solid work piece. This indicates that an annular channel will have higher levitation efficiency than a solid cylindrical channel. Experimental work is being done for both solid and hollow work piece in terms of both levitation and heating effects. Also theoretical calculations are being done for the solution of function of a complex variable to get further insight into this partitioning problem of both solid and hollow work piece.

The partitioning of levitation and heating is also influenced by the power factor. Since magnetic levitational forces arise only out of mutual inductance, there must exist

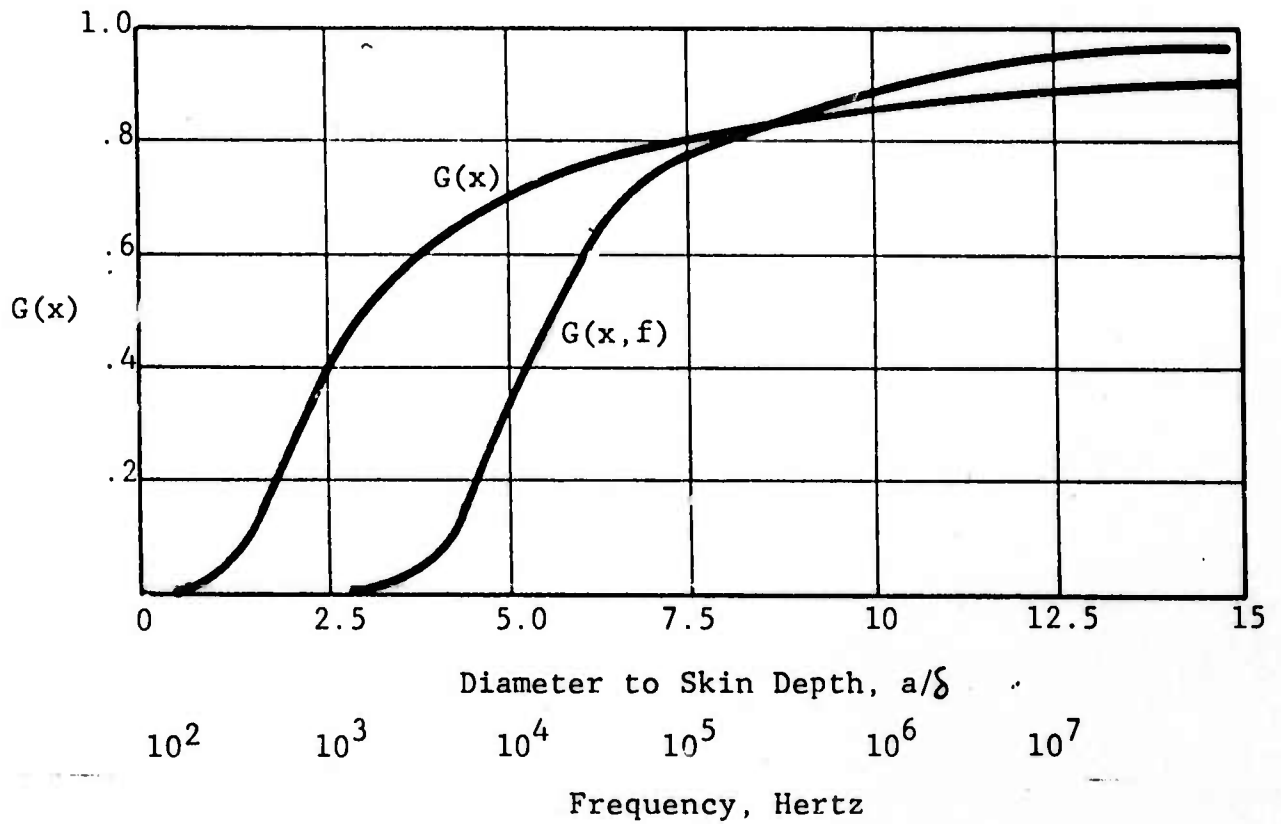


Figure 13. Levitation force efficiency as a function of workpiece diameter to skin depth and frequency.

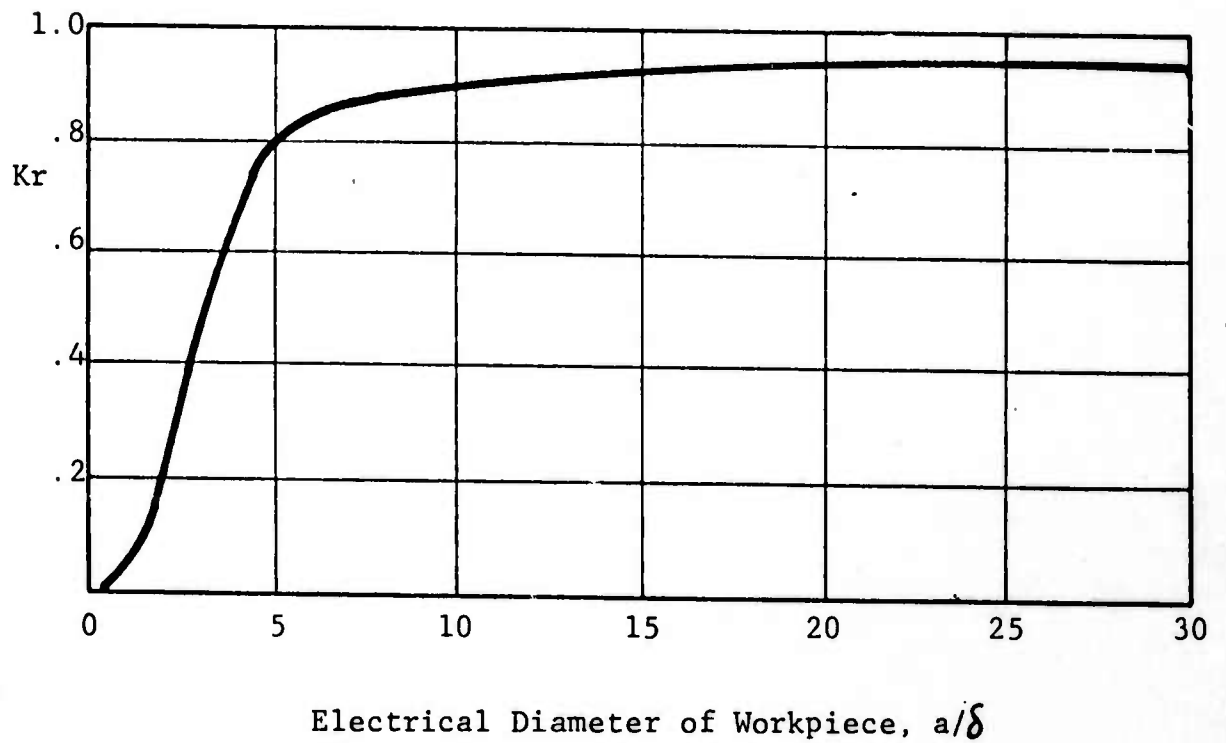


Figure 14. Resistance factor of induction heating of work-piece as a function of diameter to skin depth.

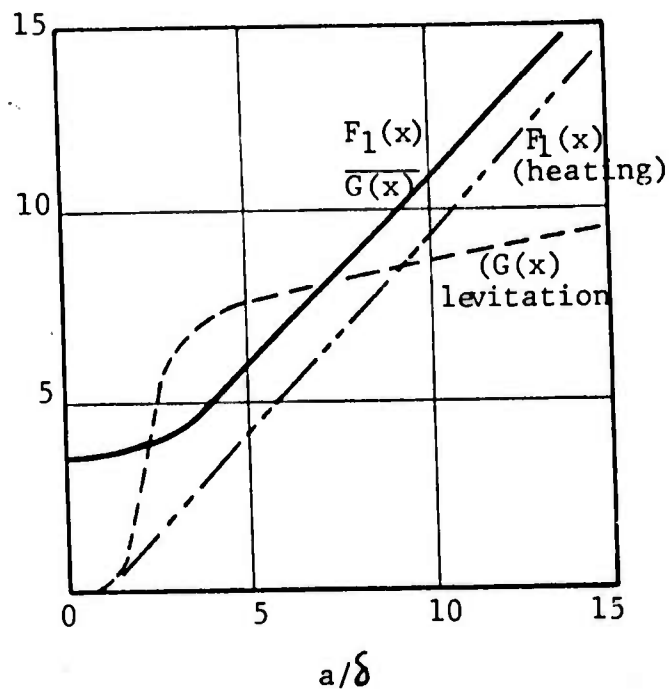
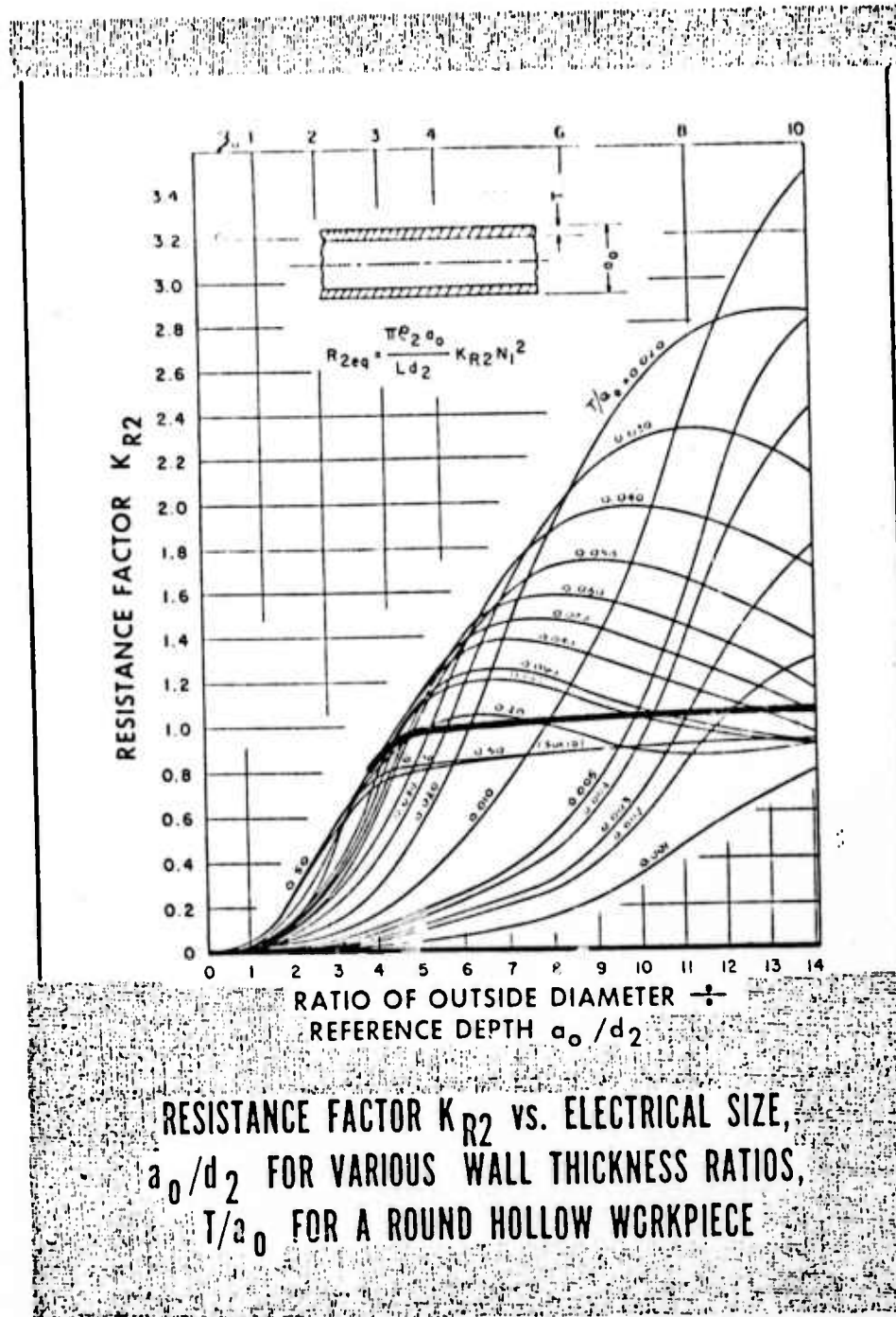


Figure 15. Partitioning of induction heating and levitation forces (after Fromm and Jehn).



(From "The Basics of Induction Heating" by Chester A. Tudbury, Rider Publication)

Figure 16

(2) contd.

a coupling coefficient which approaches a maximum of unity included in $G(x)$. It is well known that the primary coil can transfer maximum current for a given voltage when it is tuned for unity power factor. If the secondary is assumed to be wholly reactive, its current would be 90° out of phase with primary current and there would be no levitation. If the secondary is also tuned to resonance, a tremendous current would flow and there would be no induction heating because resistance is zero, yet, there should be levitation because the currents are phased. There apparently can be levitation without heating (at least cryogenically). But how do you tune a slug secondary? Furthermore, the tighter the coupling (closeness to unity) the greater the mutual interaction between the coils, therefore they cannot be tuned independently.

It is believed that the function $G(x)$ governing the efficiency of levitation should not drop off with increasing x . The work piece is becoming more inductive under these conditions, so levitation should increase if reactance is tuned out or supplied with more voltage. However, at the same time, inductive reactance becomes equal to or greater than resistance and it not only impedes secondary current but detrimentally changes its phase angle. One intuitively expects that maximum levi-

(2) contd.

tation is achieved when coupling is critical and Q is unity, Q being the ratio of stored energy to dissipate energy in a pair of coupled circuits. These requirements are yet to be determined.

Experiments are also underway to study if a multiple phase power supply can generate a better levitation than a single phase supply. A 20 KW Lepel induction heating power supply at 200 kHz is being used for a conical shaped induction coil to study this. Concurrently, a three phase alternator operating at 12 volts 500 Hertz was improvised from an automobile alternator to test levitation by multiple phase.

Attempts are also being made to build an induction coil that will generate only horizontal magnetic field so that the levitation force will be vertical everywhere.

Since it has been observed that a conduction cell is more efficient in levitating liquid than an induction cell, our approach is to use a combination of conduction and induction cells in which most of the lift will be provided by the conduction cell while the induction field will stabilize the liquid surface and provide some lift. A schematic diagram of the experimental arrangement is shown in Fig. 17. In this case the liquid-gas interface is stabilized by the application of an RF field producing a transverse magnetic field with a strong gradient.

M.H.D. Conduction Pump Valve With Lower
Surface Stabilized by A.C. Field

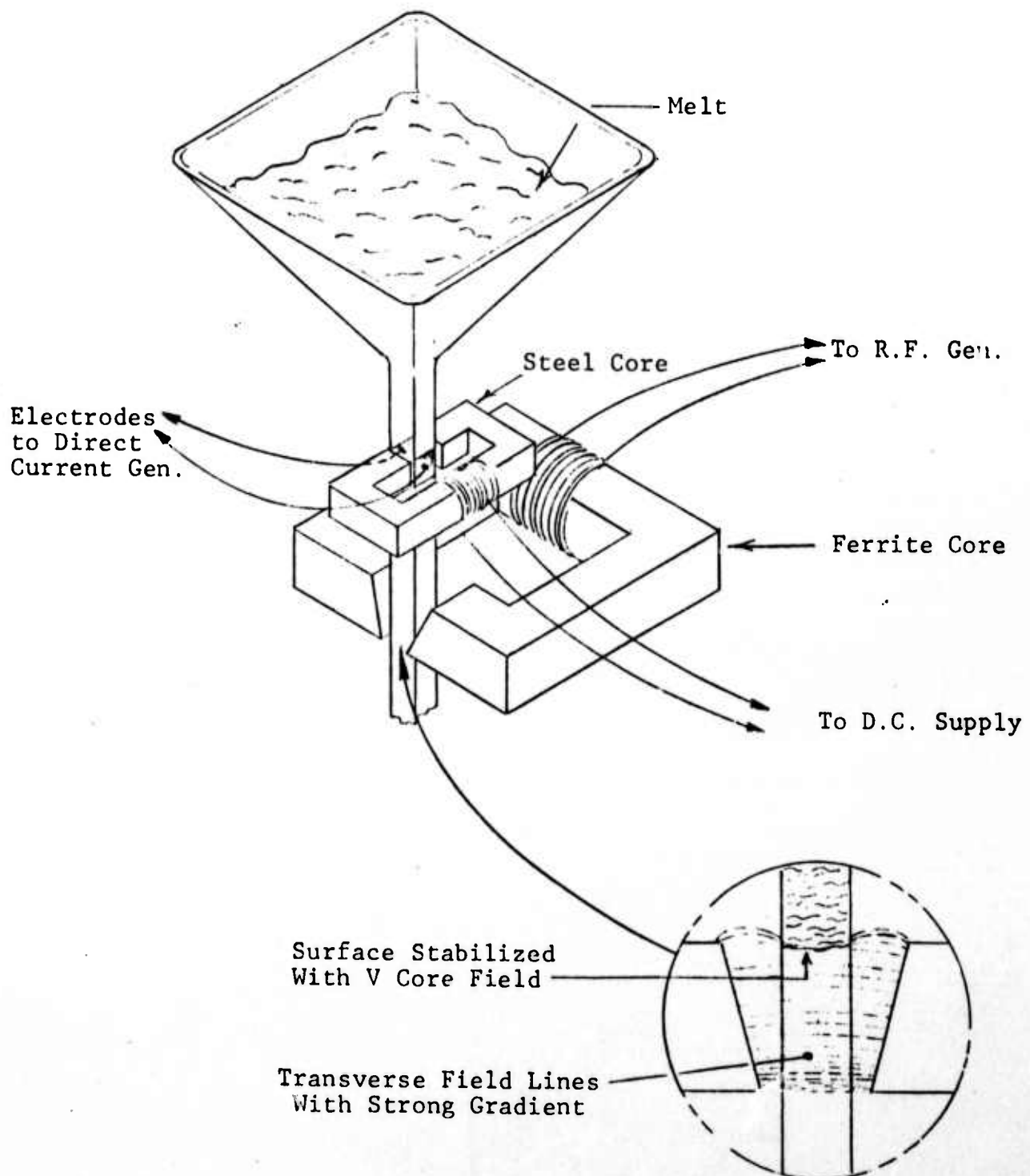


Figure 17

(2) contd.

Experiments were carried out with the fringing field of a rectangular ferrite core and the results showed that sufficient fields could be produced without difficulty to levitate small copper and brass specimens, but mercury and steel will require further effort. At 20 kHz, only the largest pieces would levitate; as the frequency was increased, the smaller sizes would float up. The mercury presents a problem because of its high density, and would require much higher field gradients. The steel appeared to be just below the levitating points as the frequency was raised to 50 kHz, but the breakdown voltage of the capacitors was reached at this point. It seems likely that an improved larger core with suitable gap dimension and a strong field gradient would be necessary for the stabilization of a mercury-air interface.

An alternative valve design was also proposed and it is shown schematically in Fig. 18. A conduction pump of circular channel having inserted cylindrical electrodes would provide an accelerator to hold back most of the head pressure. Around the lower meniscus surface of the liquid metal column would be a cup-core coil structure comprising a primary coil and a lag loop coil for interface stabilization. While only one coil element is shown having a lag loop, to comprise a single phase levitator, two or three such coil sections might be employed to expand to a two or three phase pump.

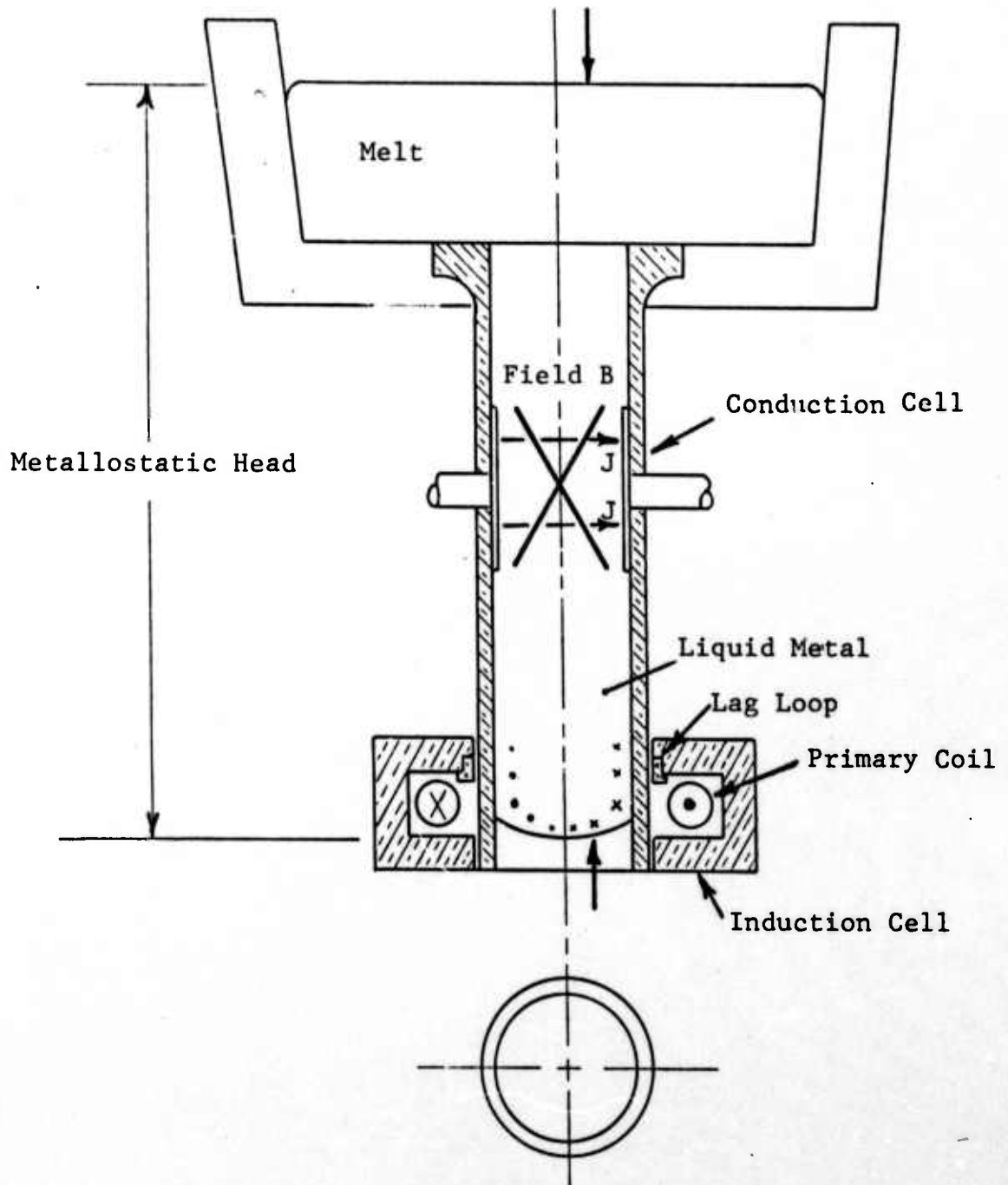


Figure 18. Proposed MHD Valve

(2) contd.

All the above experiments are currently in progress and are expected to be completed in about 6 months.

REFERENCES

- (1) E.C. Okress and D.M. Wroughton, Electromagnetic Levitation of Solid and Molten Metals, J. Applied Phys., 23, p. 545 & 1413 (1952).
- (2) E. Fromm and H. Jehn, Brit. J. Appl. Phys; 16, p. 653 (1965).

(3) Development of a Permanent Mold,

The development of permanent mold is essential for making our casting process rapid and economical. We have selected both graphite and some ceramic materials for potential permanent mold application.

Graphite.

Graphite has been considered to be the most suitable permanent mold material because of its low cost, easy machinability and above all its excellent thermal shock property. This latter is particularly important in our ferrous casting system because of high casting temperatures involved. The thermal shock resistance of a material is expressed by the parameter μ as

$$\mu = \frac{KS}{\alpha E} \quad (9)$$

where, K is thermal conductivity

S is tensile strength

α is coefficient of thermal expansion

E is modulus of elasticity

The higher the value of μ , the better is the thermal shock resistance, and graphite has higher μ than any other permanent mold material; both refractory metals and ceramic materials.

But the main problem with the graphite is its poor resistance to oxidation and erosion by molten ferrous alloys. Therefore, our primary effort has been devoted to developing a coating that will protect the graphite surface.

(3) contd.

It has been observed that the failure of all types of protective coating occurs primarily by (a) cracking and (b) spalling or peeling. These are caused mainly by the following factors:

- (a) poor bond between the coating and the graphite,
- (b) differences in the coefficients of thermal expansion of the coating and the graphite,
- (c) oxidation of the graphite underneath the coating.

On the basis of these above factors the following graphite coatings were selected for evaluation:

- (1) Ultra-temp 516
- (2) Plasma sprayed refractory oxide
- (3) Refractory oxide coating chemically bonded with refractory particles mixed with the graphite.
- (4) Diffusion bonded carbide coating with refractory oxide layer on the final surface.
- (5) Diffusion bonded carbide coating with diffusion bonded oxide layer on the final surface.
- (6) Hot pressed ceramic-graphite mix with a thin layer of graded refractory oxide on the surface.

(3) contd.

The types of graphite that have been selected to evaluate different types of coating are:

- a. Conventional graphite of varying coefficient of thermal expansion of the following types,
 - i) extruded graphite from Union Carbide Co. (ATJ, ATL & AGSR grades) and
 - ii) molded graphite from Great Lake Carbon Co. (MHLM grade)
- b. Unicast molded-to-shape graphite from Unicast Development Corporation.

Before any coating was applied, the graphite surface was sand blasted lightly with 80 mesh alundum particles to achieve mechanical bond with the coating. The surface was then cleaned by heating the graphite to about 350°F and quenching in boiling water for about 2 min. Finally it was dried in oven at 300°F for about 30 min.

A detailed discussion of the coatings and the test results are given below.

- (1) Ultra temp 516 coating - This is a proprietary coating made by Aremco Products Inc., N.Y. This material is a high strength zirconia base ceramic adhesive (heat cure) that can presumably withstand temperatures up to 4400°F.

The coating was applied by brush in thin coats several times, each coating being followed

(3) contd.

by curing at 200°F for 2 hours. It was found that during curing, the coating started to crack in some areas, and moreover, during pouring of the metal some reaction was observed in the coating.

A simple mold was designed to evaluate the coating under actual casting conditions. The mold had a rectangular cavity that made about 15 lb. castings. Graphite formed the drag while the cope was formed of sand. A step was provided on the graphite surface to test how well the coating adheres to the corners. All the castings were made of various ferrous alloys poured between 2300°F and 2800°F.

(2) Refractory oxide coating - On the basis of earlier work at Abex, alumina (Metco 101) and magnesia stabilized zirconia (Metco 210-NS) were considered to be the best coating materials because they are thermodynamically most stable oxides and chemically most non-reactive to ferrous metals. We have examined

(a) single layer

(b) double layer and

(c) four layer graded coating

(a) A single layer coating of thickness about 0.006" was applied on the graphite surface by plasma spraying. The plasma spraying was done by us-

(3) contd.

ing Metco gun at 75 volts and 400 to 500 amps. The spray distance was 4". The other parameters are: nitrogen flow rate \sim 90 CFH, hydrogen flow rate \sim 20 CFH, carrier gas flow rate \sim 40 CFH and powder feed speed dial setting -20 to 70.

A visual examination of the graphite surface after the first casting showed that the coating spalled off in the gating area where the metal first hit the mold surface.

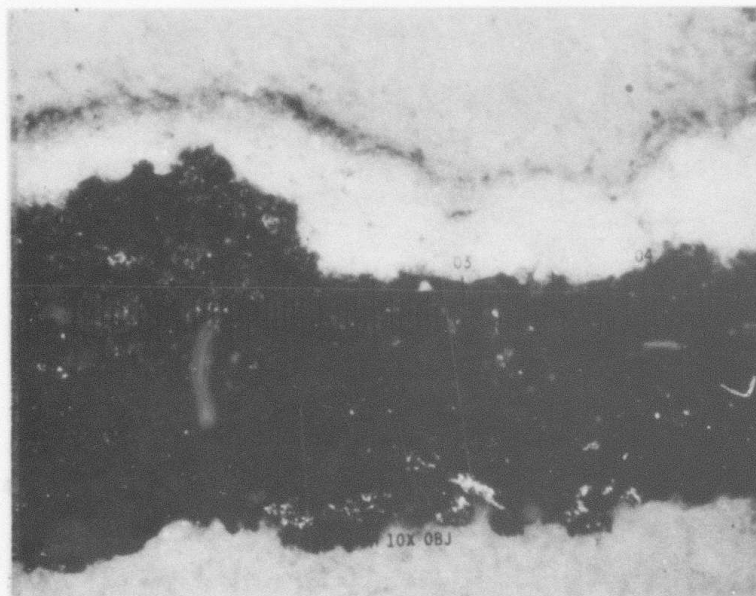
- (b) The above failure was thought to be due to poor bond between the coating and the graphite. Therefore, the bond was improved by using a bond coat of NiAl (Metco 404) before the final coat. The thickness of the bond coat was about 0.002". This produced a slight improvement; the coating started to fail in the gating area after 2 to 3 castings.
- (c) Since NiAl and MgO-ZrO_2 have different coefficient of thermal expansion, it was then decided to use compensating layers between the bond coat and the final coat to absorb the thermal stress. Two compensating layers were used, the first one

(3) contd.

consisting of a mixture of 65% NiAl and 35% MgO-ZrO₂ (Metco 413), and the second one consisting of a mixture of 35% NiAl and 65% MgO-ZrO₂ (Metco 412). The thickness of these compensating layers was about 0.002" each.

This four layer graded coating produced a great improvement, the coating started to fail after about 12 castings. The peeling of the graphite surface was noticed in the gating area and also near the edges of the step that was provided on the graphite surface. The peeled off layer was examined under microscope and it was found that it consisted of a layer of about 0.015" thick metal underneath the coating as shown in Fig. 19. It appears that the metal penetrated the oxide at cracks and spread underneath the coating. The void between the coating and the graphite was probably produced by the oxidation of the graphite surface.

- (3) Plasma sprayed coating on ceramic infiltrated graphite - Our next approach was to improve the bond between the graphite and the coating by mixing graphite with refractory particles of the same composition or other that is capable of forming chemical bonds with the coating material, so that during plasma spray, the coating will be fusion bonded with these particles.



100X

Micrograph (taken using polarized light) showing the Layer of Metal underneath the coating.

Figure 19

(3) contd.

There are several companies that manufacture Al_2O_3 mixed graphite. We examined one sample from Vesuvius Crucible Company and the material was found to be not strong enough to be used as permanent mold material. This poor strength is probably the result of the poor bond between the graphite and Al_2O_3 particles.

We contacted Unicast Development Corporation of New York who has a proprietary method of making molded-to-shape graphite. They proposed that their technique might be able to produce a strong graphite refractory composite. The following three composites were made:

- (a) NiAl mixed graphite
- (b) Al_2O_3 mixed graphite
- (c) MgO-ZrO_2 mixed graphite

About 10 to 12 volume per cent of the ceramic particles of size $-170 + 10\mu$ was mixed with the graphite in each case.

However, these ceramic infiltrated graphites also exhibited poor strength and durability. Moreover, the graphite surface had a powdery appearance that prevented any adherence with plasma sprayed coating.

- (4) Diffusion bonded carbide coating with refractory oxide coating on the final surface - One of the problems associated with the plasma sprayed coating is its inability to wet the graphite surface adequately and thereby, produce a good bond. Therefore, it was decided to change the graphite surface

(4) contd.

chemically so that the subsequent ceramic coating will have a better wettability. The most convenient method was to form metal-carbides on the graphite surface, since carbon has good diffusivity in most of the metals. The procedure is to form a thin metallic coating on the graphite surface and then form carbide by diffusion annealing. By this procedure, the carbide layer will be diffusion bonded to the graphite. On the basis of thermodynamic considerations, we selected the following three carbides:

- (a) molybdenum carbide
- (b) chromium carbide
- (c) titanium carbide

Molybdenum was deposited by plasma spraying (about 0.001" thick). Although molybdenum forms some oxide (~5%) during plasma spraying in the air, it was considered not to be harmful.

Several procedures for coating with titanium were investigated of which the following two methods were selected:

- (a) vapor deposition and
- (b) pack metallizing

Vapor deposition of titanium was done at AMMRC (Army Materials and Mechanics Research Center), Mass. by vapor-

(4) contd.

ization of pure titanium wires under vacuum. Pack metallizing was done by Chromalloy Research and Technology, New York by packing graphite specimen with titanium powder and carrier gas in a closed crucible and heating at around 2000°F inside a furnace. The exact coating thickness of these two processes is not known but probably of the order of 4×10^{-5} in ($= 1 \mu$).

Chromizing of the graphite samples was also done by pack metallizing technique at Chromalloy Research, New York. The coating thickness was probably about 4×10^{-5} in.

For carbide formation, all the specimens were diffusion annealed at 2000°F for 1 hour in a vacuum furnace. After diffusion annealing, x-ray diffraction analysis of the graphite surface was done to examine the carbide formation and the results are shown in Table I.

It can be seen that pack metallizing is the most successful technique for carbide formation. Although chromium has formed complete carbide, titanium has formed some TiN along with TiC . The appearance of strong carbon lines in the diffraction pattern indicates that the carbide layer was very thin. The vapor deposition technique is not successful due to formation of excessive oxides, and moreover, it is an extremely slow process.

Table I
RESULTS OF X-RAY DIFFRACTION ANALYSIS

<u>Coating Before Diffusion Annealing</u>	<u>Surface Constituents</u>
(1) Chromium by pack metallizing	Cr ₂₃ C ₆
(2) Titanium by pack metallizing	TiC - Major TiN - Major C - Major TiO ₂ - Minor
(3) Titanium by vapor deposition	C - Major TiO ₂ - Minor Ti ₄ O ₇ - Minor
(4) Molybdenum by plasma spray	Mo - Major MoC - Minor γ-MoC - Minor

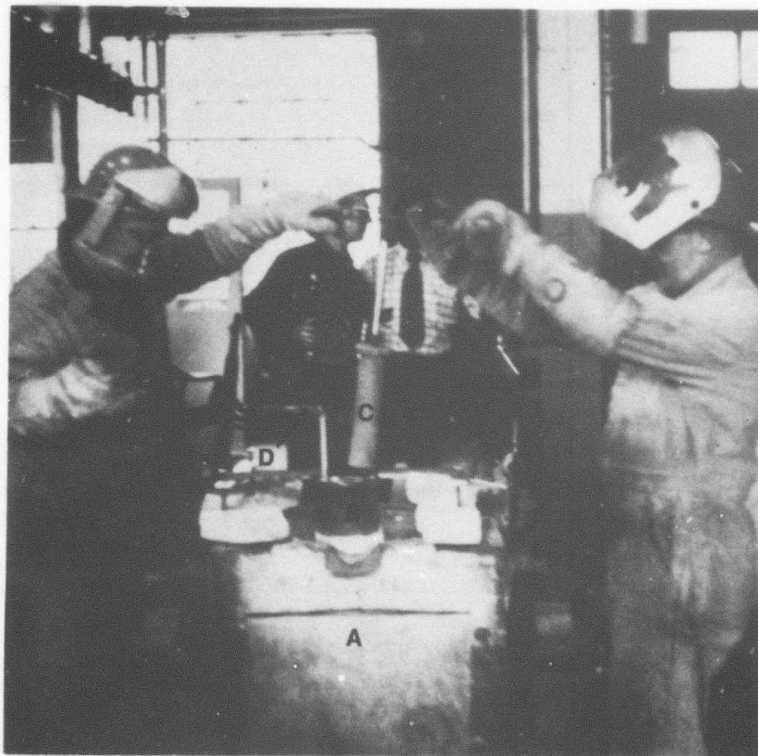
(4) contd.

The plasma spray technique is partly successful. The lack of formation of MoC is probably due to insufficient heat treatment. Therefore, a thinner coating and a longer annealing are required for complete carbide formation.

In any event, two samples were made of each of the above processes and one of them was coated with a single layer of $MgO-ZrO_2$ while the other was coated with 4 layer graded $MgO-ZrO_2$, using NiAl as the bond coat. One titanium carbide coated sample, however, was coated with a single layer of TiO_2 .

For the evaluation of these carbide coatings we decided to use dip test instead of pour test, since dip test is faster and less expensive. Although dip test and pour test are not identical for mold evaluation, the thermal shock resistance and mold-metal reaction can be evaluated equally in both the tests. However, in our case the dip test has been used only for screening purpose. The best coating will be used in actual mold for pour testing for final evaluation. Cylindrical samples of 2-1/2" dia. x 8" long size with insertable steel rod at one end was prepared for the dip test.

The dip test arrangement is shown in Fig. 20, where A is an induction furnace containing molten metal at a constant temperature of 2350°F with power on. Cast iron of C-3.5% and Si-2.0% composition was used for the test.



Dip Test Experiment
Figure 20

(4) contd.

B is a cylindrical steel chamber with the bottom open and the top covered with a transite lid. C is the cylindrical specimen that is suspended by a handle bar on one end and inserted into the chamber through its top. D is the gas port that leads argon gas into the chamber to flush it continuously. This inert atmosphere is maintained to prevent any slag formation. A gap of about 2" is provided between the metal surface and the bottom of the chamber for the outlet of argon. The specimen was dipped into the metal by about 5" and held there for several seconds until the surface reached the temperature of the melt. It was then pulled out and allowed to cool to about 1000°F and then dipped again. This cycle was repeated 10 times before it was cooled to room temperature for visual examination. The results of the dip test are shown in Figure 21.

As can be seen, most of the coatings failed before 50 cycles were completed except for only two. After 50 cycles, the 4 layer graded ZrO_2 coating on Cr-carbide surface still looked good, whereas, the single layer ZrO_2 coating on Mo-carbide surface looked fairly good. These two coatings are being evaluated by pour test in graphite molds. The cause of failure of other coatings may probably be attributed to insufficient formation of carbides.

DIFFUSION BONDED CARBIDE COATING

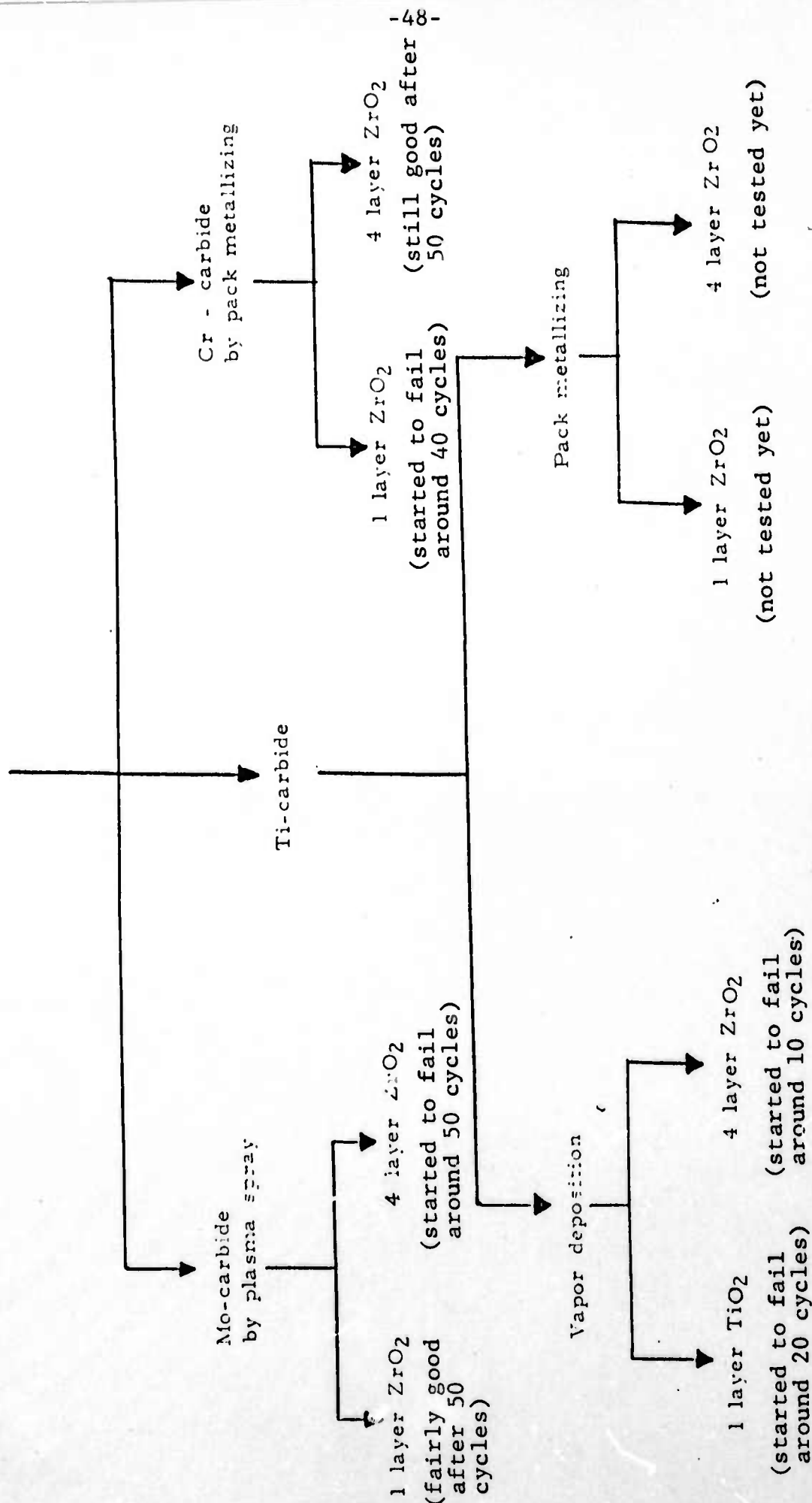


Figure 21

- (5) Diffusion bonded carbide coating with diffusion bonded oxide layer on the final surface - The next step taken was to improve the bond between the carbide surface and the oxide coating by forming a diffusion bond between the two. This was accomplished by plasma spraying a pure metal on the graphite surface and then diffusion annealing in a controlled oxidizing atmosphere. A diffusion bonded carbide layer was formed at the graphite surface and a diffusion bonded oxide layer on the final surface. On the basis of thermodynamic considerations, titanium was selected as the coating material. The experimentations to form this carbide-oxide layers are still in progress.
- (6) Hot pressed ceramic-graphite mix with graded refractory oxide on the surface - Instead of plasma spray, attempts are being made to hot press a thin layer (about 0.01") of graded MgO-ZrO_2 on the graphite surface. Since pure graphite does not bond with ZrO_2 too well, attempts are being made to make different ceramic-graphite mix so that ZrO_2 layer will bond strongly with this substrate. The Norton Company's ZRBSC-M (a hot pressed zirconium boride-silicon carbide-graphite) has been selected as the base material because of its high resistance to thermal shock. Problems were being encountered in selecting hot pressing temperature because of a large difference in this temperature for ZrO_2 and ZRBSC-M. This work is still in the development stage and is expected to be completed very shortly.

CERAMIC MATERIALS:

Besides graphite, we are also investigating the following hot pressed ceramic materials for permanent mold application:

- (a) Silicon nitride (from Norton Co.)
- (b) Boron nitride (from Carborundum Co.)
- (c) Zirconium diboride (")
- (d) Boride "Z" (")

These materials are being evaluated by pour test (small specimens are embedded in a sand mold and large specimens are used as chill plates underneath open cylindrical sand molds), both in coated (single layer of $MgO-ZrO_2$) and uncoated state. The coating on silicon nitride failed after 2 castings, whereas the uncoated area showed very little reaction even after 5 castings. The coating on boron nitride started to fail after 5 castings and the uncoated area showed a slow reaction with the metal after each casting. Zirconium diboride showed an extremely poor thermal shock resistance and cracked during every pouring. The coating on boride "Z" was unsuccessful also and the uncoated area showed some reaction with the metal.

Silicon oxinitride will also be evaluated for a permanent mold application in the future.